THERMAL DECOMPOSITION OF MAGNETITE DUE TO IMPACT HEATING. K. Kurosawa[1], G. S. Collins[2], T. M. Davison[2], T. Okamoto[1], K. Ishibashi[1], and T. Matsui[1], [1]Planetary Exploration Research Center, Chiba Institute of Technology, (2-17-1, Tsudanuma, Narashino, Chiba 275-0016, Japan; kosuke.kurosawa@perc.it-chiba.ac.jp), [2]Impact and Astromaterials Research Centre, Dept. of Earth Sci. Eng., Imperial College London.

Introduction: Magnetite (Fe_3O_4) is one of major minerals in a hydrated asteroid Ryugu [1] and CI and CM chondrites [e.g., 2]. Since thermal decomposition of magnetite, Fe_3O_4 -> $3FeO + 1/2O_2$, occurs at a relatively low temperature (<2,000 K depending on oxygen fugacity), magnetite might behave as an oxidizing agent in impact chemistry on carbonaceous asteroids. However, the decomposition behavior of magnetite due to impact heating is not well understood.

Remote sensing observations of Ryugu conducted by the Hayabusa2 spacecraft [3] and the sample analyses of Ryugu particles [1] revealed that the carbonaceous asteroids have substantial porosity. Compaction of porosity can dramatically enhance the degree of impact heating [e.g., 4]. Although the ε–α porosity compaction model for shock physics codes is well established [5], experimental validation of its predictions of post-shock residual temperature, which is the most influential parameter of impact chemistry, has been lacking.

For the two motivations above, we studied impact devolatilization of magnetite using magnetite powder, i.e., a purely Fe–O system, as a first step. We are able to easily produce a pellet with a porosity. Since the phase diagram of the Fe–O system is well-established [e.g., 6], we can estimate the residual temperature field based on the total O_2 production N_{O2}. In this study, we investigated N_{O2} as a function of impact velocity v_{imp} and initial porosity ϕ_0. Then, we compared the experimental results with the heated mass calculated by the iSALE shock physics code [5, 7, 8]. As magnetite decomposes above 1,890 K [6], any O_2 production after impact provides direct evidence that the shocked targets were heated to above 1,890 K.

Methods: We conducted both laboratory experiments and shock physics modeling as follows.

Laboratory impact experiments. We investigated impact decomposition of magnetite with a two-stage light gas gun at the Planetary Exploration Research Center (PERC) of Chiba Institute of Technology, Japan [9]. We used an Al_2O_3 sphere as a projectile with a diameter of 2 mm. A nylon slit sabot [10] was used for accelerating the projectile. ϕ_0 and v_{imp} were varied from 51% to 79% and from 3.19 km s^{-1} to 7.04 km s^{-1}, respectively. We only conducted vertical impacts. The impacts occurred in a fully-open system filled with Ar gas with a total pressure of 500 Pa. To avoid the chemical contamination from the gun operation, the two-valve method [11, 12] was used. The impact-generated gases were measured with a quadrupole mass spectrometer (QMS; Pfeiffer, Prisma plus QMG220). A calibration experiment was also conducted with air to quantify N_{O2}.

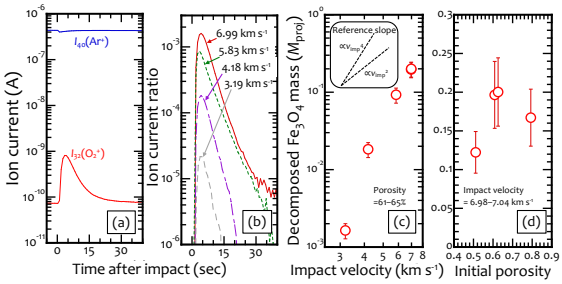

Figure 1. Experimental results. (a) A raw data of shot #542. (b) Ion current ratio to I_{40} as a function of time. The corresponding v_{imp} are shown beside the lines. (c) and (d) Decomposed magnetite mass as a function of v_{imp} and ϕ_0, respectively.

Shock physics modeling. We conducted standard impact simulations, which model a vertical impact of a spherical projectile onto a flat target under the same conditions as the experiments except for no ambient gas in the simulation. The Tillotson EOS [13] for Al_2O_3 [14] was used to describe the projectile. We constructed a new parameter set for ANEOS [15] to describe the hydrodynamic and thermodynamic response of magnetite based on known shock Hugoniot data [16] and thermo-elastic properties [17]. We also used the ε–α model to treat the effect of pore collapse on impact heating. Note that no strength model was employed in the simulations.

Results: Figure 1a shows an example of raw experimental data. The ion current for the mass number $M/Z = i$ is denoted as I_i. A sudden rise in $I_{32}(O_2^+)$ was observed, showing that we detected O_2 production from the magnetite pellet due to impact heating. In contrast, we confirmed that $I_{40}(Ar^+)$ was stable during the measurement, allowing us to quantify N_{O2} by referencing to the ion current ratio of I_{32} to I_{40}. Figure 1b shows the ion current ratios of I_{32} to I_{40} at 4 different values of v_{imp}. We clearly detected an O_2 generation even at 3.19 km s^{-1}. Figures 1c & d show decomposed magnetite mass calculated from N_{O2} as a function of v_{imp} (c) and ϕ_0 (d). We found that N_{O2} strongly depends on v_{imp} ($\propto v_{imp}^4$), suggesting that the heated mass cannot be

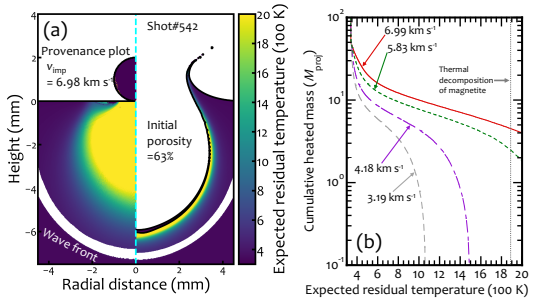

Figure 2. An example of the iSALE results. This simulation corresponds to the shot #542. We show both a provenance plot (a) and a snapshot at 2.9 μs after the impact. The color bar indicates expected residual temperature (See text). (b) Heated mass distribution. The corresponding v_{imp} are shown beside the lines. The temperature at the thermal decomposition of magnetite is shown as the dashed grey vertical line.

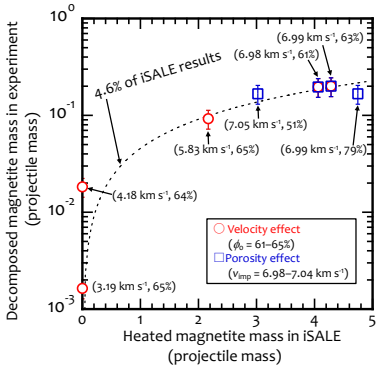

Figure 3. Comparison between the laboratory and numerical experiments. The impact velocity and the initial porosity of the target of each experiment indicate beside the data point. The black dashed line shows the 4.6% of the iSALE results.

scaled simply by the kinetic energy of the impact. The porosity effect on N_{O2} is not clear, possibly due to a trade-off between the lower specific mass per unit volume and the higher heating efficiency with increasing ϕ_0.

Figure 2 shows an example of the iSALE results. We estimated "expected" residual temperature T_{res} after decompression down to 10^5 Pa by assuming an isentropic release from the peak shock states (Fig. 2a). Figure 2b shows the cumulative mass heated to a temperature higher than T_{res} as a function of T_{res}. Figure 3 shows a comparison between the experimental and iSALE results. Decomposed magnetite masses were plotted against the heated target mass having T_{res} > 1,890 K in the iSALE simulations. We found that iSALE reproduced a decomposition trend at v_{imp} higher than 5.8 km s^{-1} if we multiply the iSALE results by a factor of 4.6% regardless of v_{imp} and ϕ_0. However, the iSALE results cannot explain the O_2 generation at v_{imp} <4.2 km s^{-1} observed in the laboratory experiments even though we considered the enhancement of the impact heating due to pore collapse.

Discussion & Conclusions: We demonstrated a system to investigate thermal decomposition of magnetite in porous targets. We will explore the decomposition behavior of magnetite under various oxygen fugacity in the near future.

The iSALE results at high v_{imp} (Fig. 3) indicate that iSALE and the ε–α model captures well the controlling physics of impact heating in porous targets. The factor of 0.0456 could correspond to the actual decomposed fraction in the heated mass above 1,890 K in the experiments. Some local heating mechanism(s), which were not accounted for in the continuum iSALE calculations, might cause the thermal decomposition of magnetite in the experiment at low v_{imp}. Since the decomposed mass of magnetite reaches a few % of the projectile mass at v_{imp} = 4.2 km s^{-1}, which is close to an average v_{imp} in the main asteroid belt [18], such local heating might be the origin of thermal metamorphism recorded in carbonaceous chondrites [e.g., 19].

Acknowledgments: This work was supported by ISAS/JAXA as a collaborative program with the Hypervelocity Impact Facility. We also thank the developers of iSALE, including K. Wünnemann, B. Ivanov, J. Melosh, and D. Elbeshausen. GSC and TMD were supported by UK STFC grant ST/S000615/1.

References: [1] Nakamura, T. et al. (2022) *Science* 10.1126/science.abn8671. [2] Britt, D. T. et al. (2019) *Meteoritics & Planet. Sci.* (*MaPS*), *54,* 2067. [3]Watanabe, S. et al. (2019) *Science* 364, 268. [4] Ahrens, T. J. & O'Keefe, J. D. (1972), *The Moon*, **4**, 214. [5] Wünnemann, K., et al. (2006) *Icarus*, 180, 514. [6] Hidayat, T. et al. (2015) *CALPHAD* 48, 131. [7] Amsden, A. A., et al. (1980) *LANL Report* LA-8095. 101 p. [8] Ivanov, B. A., et al. (1997), *IJIE*, 20, 411. [9] Kurosawa, K. et al. (2015) *Journal of Geophysical Research Planets* (*JGR*), 120, 1237. [10] Kawai N. et al. (2010) *RSI*, **81,** 115105. [11] Kurosawa, K. et al. (2019), *Geophysical Research Letters* (*GRL*), **46**, 7258. [12] Kurosawa, K. et al. (2021) *Communications Earth & Environment* 2, 146. [13] Tillotson, J. H. (1962) *Technical Report GA-3216*, General Atomic Report. [14] Kurosawa, K. et al. (2021) *GRL* 48, e2020GL091130. [15] Thompson, S. & Lauson, H. (1972) *SNL Report*, SC-RR-71 0714:113p. [16] Marsh, S. P. (1980). *LASL shock Hugoniot data*. University of California Press. [17] Siersch, N. C. et al. (2022) *American Mineralogist* 10.2138/am-2022-8571. [18] Bottke, W. F. (1994) *Icarus* 107, 255. [19] Velbel, M. A. & Zolensky, M. E. (2021) *MaPS* 56, 546.